Plastic scintillator based PET detector technique for proton therapy range monitoring: A Monte Carlo study

Antoni Rucinski1, Jakub Baran1, Magdalena Garbacz1, Monika Pawlik-Niedzwiecka1,2 and Pawel Moskal2
On behalf of the J-PET collaboration

***Abstract*—Currently a positron emission tomography (PET) based on novel, cutting-edge technology is developed by the Jagiellonian-PET (J-PET) collaboration. In this contribution, the principle of plastic scintillator based detector system, J-PET and the investigation of its feasibility for proton beam therapy range monitoring will be presented. Results of Monte Carlo simulation studies aiming at the characterization of secondary radiation induced by a proton beam in a PMMA phantom and detected by the J-PET scanner will be shown. Accounting for detector acceptance and PET-gamma detection efficiency in the plastics the diagnostic J-PET scanner can acquire 1.7×10^{-5} PET-gammas per primary proton. The J-PET detector configurations and signal acquisition during and after the therapy is discussed.**

I. Introduction

Proton beam therapy (PBT) is a cancer radiotherapy technique that enables precise delivery of the dose to the tumor and preservation from irradiation of healthy tissues, as the maximum dose is deposited at the end of the proton range in the Bragg peak [1]. To ensure complete coverage of the tumor in the presence of uncertainties, safety margins around tumor in the order of 3.5% of proton range in patient body are applied causing irradiation of surrounding healthy tissue with the therapeutic dose. Beam range monitoring techniques further could help in decreasing target volume safety margins and apply new treatment protocols in the clinic [2]. Such techniques exploit secondary radiation induced by the proton beam and emitted from the irradiated area during or just after the treatment. Various centres investigated Positron Emission Tomography (PET) [3], [4], [5], prompt photon monitoring techniques [6], [7], and secondary charged particles tracking [8], [9] in a clinical context. The secondary emitters can be detected by in-beam, off-beam or after-treatment PET. Through Monte Carlo simulations the signal can be related to the range of the primary proton beam giving insight on planned and delivered dose [10].

The Institute of Nuclear Physics PAN in Krakow, the first facility in Poland, offers proton beam therapy to head and neck and pediatric cancer patients. Two rotational gantries equipped with pencil beam scanning and an eye treatment room are in clinical operation since October 2016, and until November 2018 more than 120 patients have been treated.

At the Jagiellonian University (UJ) in Krakow a cost effective method for total-body PET has been built and is currently being tested. The first generation prototype of the time-of-flight (TOF) based, diagnostic J-PET scanner consists of three cylindrical layers of EJ-230 (ELJEN Technology) plastic scintillator strips ($7\times19\times500\,\mathrm{mm}^3$) connected to vacuum tube photomultipliers [11], [12]. The efficiency of the prototype is currently being investigated. J-PET is used for fundamental physics studies on positronium imaging, quantum entangelment [13], [14] and studies of discrete symmetries in nature [15], [16], [17]. The second generation modular J-PET prototype is currently under construction [18]. A single detection module of the strip-based PET is assembled out of 13 long scintillator strips. Photons interact with the plastic scintillator through Compton scattering and produce light pulses in a strip propagating to the strip edges and converted into electric signals by silicon photomultipliers (SiPM). The signals are read-out by fast, customized on-board front-end electronics with coincidence resolving time (CRT) of about 400 ps [19], [20], [21]. Such a modular detector design is lightweight and portable enabling easy configuration and installation of various setups [22], [23].

In this contribution the preliminary results of the simulation study investigating the feasibility of J-PET detector technique for PBT range monitoring are presented. GATE [24] Monte Carlo simulations are used to study the production of PET-gamma in a PMMA phantom and to characterize the J-PET detector sensitivity, i.e. PET-gamma signal in J-PET detector per incident primary proton. Different setup configurations built by J-PET modules are investigated: a full ring and a dual head approach.

II. Materials and Methods

The geometry of J-PET module consisting of 13 long scintillator strips of $6\times24\times500$ mm^2 rectangular cross section was implemented in GATE. Commercial plastic scintillators BC-404 from Saint-Gobain wrapped with two layers of a light impermeable foil were used. The expected efficiency for Compton interaction of a back-to-back annihilation photon in the plastic is about 10%. The geometry of silicon

[1] Institute of Nuclear Physics PAN, 31-342 Krakow, Poland
Email: antoni.rucinski@ifj.edu.pl, antoni.rucinski@gmail.com
[2] Faculty of Physics, Astronomy and Applied Computer Science, Jagiellonian University, 30-348 Krakow, Poland

978-1-5386-8494-8/18/$31.00

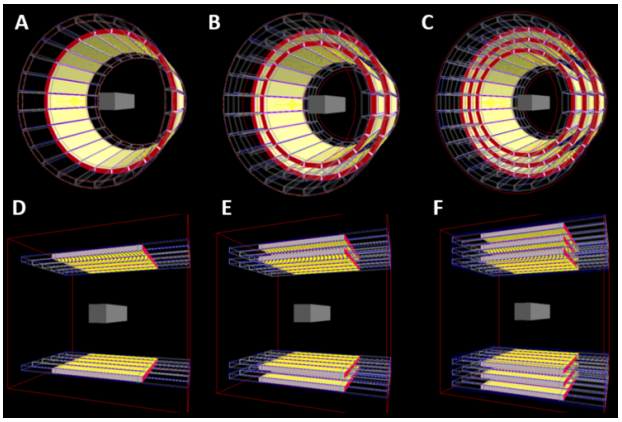

Fig. 1. Scanner geometry setups.

photomultupliers and front-end electronics was also implemented but optical signal propagation in the scintillators and electronic signal acquisition were not simulated. Six different PET system geometries composed of the J-PET modules were implemented: three ring systems (a barrel) and three dual head configurations. Single, double and triple layers systems (Tab. I and Fig. 1) were investigated as expected signal detection probability increases with the number of layers. Solid angle of single layer barrel and dual-head systems are: 5.03 [sr] and 3.39 [sr], respectively. The number of modules in a ring scanner depends on the barrel diameter, i.e. barrel bore (Tab. I). The dual head system consist of five detection modules independent of the number of layers applied. A PMMA phantom (100 x 100 x 400 mm^3) with the 74 eV PMMA ionization potential was positioned isocentrically inside the detector system. The GATE toolbox version 8.1[24], [25] based on Geant4 version 10.4[26] was used for the simulation. The QGSP_BIC_HP_EMY physics list (recommended by developers) which includes both electromagnetic and hadronic interactions models was applied [27].

MC simulations of a point-like source placed isocentrically in a PMMA target positioned in the center of the J-PET detector field-of-view (FOV) were performed to study the detector sensitivity. 10^6 back-to-back gammas were emitted isotropically from the source. Sensitivity was calculated for all investigated setup configurations as a ratio of the number of detected coincidences to the number of emitted photon pairs.

Full simulations were performed to study secondary PET-gamma production and detector response for various detector designs. The PMMA target was irradiated with 10^7 primary protons at 150 MeV. Proton beam model used clinically in Krakow proton beam therapy centre was implemented in GATE and used for simulations [28], [29]. Using GATE actors we scored the dose deposited by the proton beam, production of secondary particles namely gammas, electrons, protons, and neutrons, and positron-electron annihilation events. Production, annihilation events and dose were transversely integrated and binned to 2 mm grid. An in-house developed software tools implemented in ROOT scripting environment were used

TABLE I
SCANNER GEOMETRY SETUPS.

Scanner geometry	Number of J-PET layers	Number of J-PET modules	Isocenter to detector distance [mm]*
A	1	24	382
B	2	44	318, 382
C	3	72	318, 382, 446
D	1	10	300
E	2	20	300, 368
F	3	30	300, 368, 436

* Distance from the isocenter to the surface of the first, second and third J-PET detector layer

to find coincidence events under the condition that each of the two gammas produced by the same annihilation deposited more than 150 keV energy in the scintillator by Compton scattering, which is experimentally used as time-over-threshold (TOT) trade-off. Beam time duration was 1 ms. We calculated two different cumulative quantities: (i) by integrating the J-PET detector signal (produced by decays) over the first five minutes after the irradiation and (ii) by summing all decay events regardless of the time stamp. The signal was integrated transversally along the phantom to build the activity profile as a function of depth along the beam axis. The dose deposition profile was compared with the PET activity profile. The detector was idealized as scattered coincidence events as well as time coincidence window were not considered in the analysis.

TABLE II
DETECTION SENSITIVITY RESULTS.

Scanner geometry	Number of detected coincidences	Detection efficiency in %
A	2676	0.27
B	6664	0.67
C	9447	0.95
D	1414	0.14
E	2958	0.30
F	4419	0.44

III. RESULTS

Tab. II shows the detection sensitivity for all tested system configurations. Depending on the number of detector layers and modules, the sensitivity ranges from 0.27% to 0.95% and from 0.14% to 0.44% for a barrel and for a dual head systems, respectively.

The full simulations gave the number of detected coincidence events for 10^7 primary protons. The number of detected coincidences summing all decay events regardless of the decay time stamp for single, double and triple layer barrel setup is 170, 758, 1361, and for dual head setup 68, 264, 538, wherease integrating signal within the first five minutes after the irradiation the signal is 78, 342, 441, and 21, 108, 108, 242, respectively. Fig. 2 shows the PET activity profiles built by summing all decay events regardless of the decay time stamp from annihilation points obtained from MC simulations together with the dose deposited in the PMMA phantom.

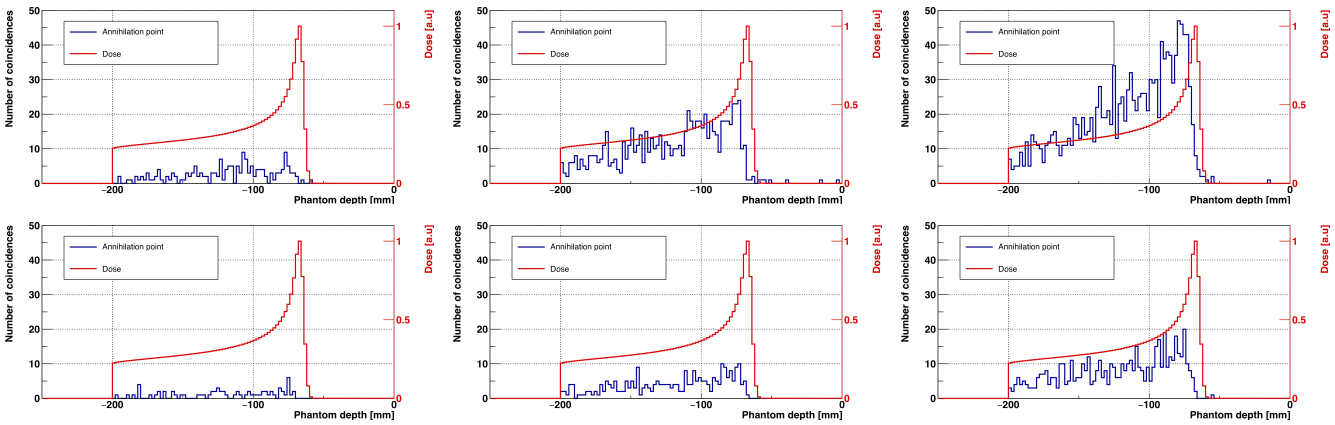

Fig. 2. The dose deposition profile (red) and PET activity profile (blue) build for a barrel (top) and dual-head setup for single (left), double (middle) and triple (right) layer J-PET configurations.

IV. Discussion

J-PET setup configurations built with a modular J-PET detector system were tested regarding potential application in proton therapy range monitoring. The sensitivity of the J-PET detector estimated from MC simulations is on the per mille level. A diagnostic barrel design allows the detection of 1.7×10^{-5} back-to-back coincidences per impinging primary proton. The sensitivity increases with the number of detector layers and is smaller for the dual-head design than for a barrel due to smaller solid angle (see Fig. 2). The low efficiency of the plastic scintillators for detection of photons originating from decay with respect to crystals can be compensated by the solid angle of the detector and increasing the number of detector layers.

In the presented work, 10^7 primary protons were simulated. The number of protons in the last slice of a typical clinical proton plan can be higher than this figure by one order of magnitude or more. Therefore, we expect that the signals would be even higher that the results we reported in this contribution. The abundance of events and thus the signal obtained in the detector is patient and site specific as it depends on the location of the tumor (shape and size) and is determined by the energy and number of protons used in the treatment plan per pencil beam. The signal can be increased by optimizing the detector design and the signal acquisition time during or after the irradiation (off-beam, inter-spill or combination of both) as we have shown for single, double and triple layer systems and two signal integration times (five minutes and summing all the events). The activity profiles illustrated in Fig. 2 are built from the original annihilation positions given by MC simulations. In fact, to reproduce the true J-PET detector signal in MC simulations, the simulated J-PET module characteristics should account for the achievable time resolution of calculation of Compton interaction points in the plastic with the TOF technique, optical signal propagation and conversion characteristics specific to SiPM and front-end electronic characteristic (dead-time and TOT trade-off). The precise characteristics of the investigated modular J-PET have not been experimentally investigated yet and several assumptions were done in this work in order to estimate the signal that can be achieved using the proposed setup geometry. The investigated designs are likely not the ultimate solutions which would be employed in clinics and the feasibility of their integration into the proton therapy treatment room is beyond the scope of this manuscript.

Our future aims include detector characterization and the application of image reconstruction algorithms and correction factors (normalization, attenuation, random and scatter corrections). We will compare the possible achievable sensitivity with state-of-the-art crystal based PET systems. To assess the feasibility of modular J-PET technology for range monitoring, the expected accuracy of Bragg-peak range determination must be estimated. The experimental validation of MC simulations is planned in the Krakow proton beam therapy facility.

V. Conclusion

We have investigated the possible achievable response of the plastic scintillator based J-PET detector in MC simulations. The results of the study are promising, but further work is required to demonstrate the clinical potential of J-PET detector for proton beam therapy range monitoring.

Acknowledgment

Research was supported by the National Centre for Research and Development (NCBiR), grant no. LIDER/26/0157/L-8/16/NCBR/2017. JB and MG acknowledge the fellowship with project no. POWR.03.02.00-00-I013/16

References

[1] M. Durante, R. Orecchia, and J. S. Loeffler, "Charged-particle therapy in cancer: clinical uses and future perspectives," *Nature Reviews Clinical Oncology*, vol. 14, pp. 483 EP –, 03 2017. [Online]. Available: http://dx.doi.org/10.1038/nrclinonc.2017.30

[2] H. Paganetti, *Proton Therapy Physics*, J. G. Webster, S. Tabakov, and K.-H. Ng, Eds. Boston, USA: CRC Press Taylor & Francis Group, 2012, vol. 103.

[3] M. G. Bisogni *et al.*, "INSIDE in-beam positron emission tomography system for particle range monitoring in hadrontherapy," *Journal of Medical Imaging*, vol. 4, no. 1, p. 011005, 2016. [Online]. Available: https://doi.org/10.1117/1.JMI.4.1.011005

[4] J. Bauer *et al.*, "Implementation and initial clinical experience of offline PET/CT-based verification of scanned carbon ion treatment," *Radiotherapy and Oncology*, vol. 107, no. 2, pp. 218–226, 2013. [Online]. Available: http://dx.doi.org/10.1016/j.radonc.2013.02.018

[5] V. Ferrero, E. Fiorina, M. Morrocchi *et al.*, "Online proton therapy monitoring: clinical test of a Silicon-photodetector-based in-beam PET," *Scientific Reports*, vol. 8, no. 1, p. 4100, 2018. [Online]. Available: http://www.nature.com/articles/s41598-018-22325-6

[6] J. Krimmer, D. Dauvergne, J. M. Létang, and Testa, "Prompt-gamma monitoring in hadrontherapy: A review," *Nuclear Instruments and Methods in Physics Research, Section A: Accelerators, Spectrometers, Detectors and Associated Equipment*, vol. 878, no. May 2017, pp. 58–73, 2018. [Online]. Available: http://dx.doi.org/10.1016/j.nima.2017.07.063

[7] C. Richter *et al.*, "First clinical application of a prompt gamma based in vivo proton range verification system," *Radiotherapy and Oncology*, vol. 118, no. 2, pp. 232–237, 2016. [Online]. Available: http://dx.doi.org/10.1016/j.radonc.2016.01.004

[8] G. Battistoni *et al.*, "Measurement of charged particle yields from therapeutic beams in view of the design of an innovative hadrontherapy dose monitor," *Journal of Instrumentation*, vol. 10, no. 2, 2015.

[9] A. C. Kraan, "Range Verification Methods in Particle Therapy: Underlying Physics and Monte Carlo Modeling," *Frontiers in Oncology*, vol. 5, no. July, pp. 1–27, 2015. [Online]. Available: http://journal.frontiersin.org/Article/10.3389/fonc.2015.00150/abstract

[10] K. Parodi and W. Enghardt, "Potential application of PET in quality assurance of proton therapy." *Physics in medicine and biology*, vol. 45, no. 11, pp. N151–N156, 2000.

[11] P. Moskal, S. Niedźwiecki *et al.*, "Test of a single module of the J-PET scanner based on plastic scintillators," *Nucl. Instr. and Meth. A*, vol. 764, pp. 317–321, 2014.

[12] S. Niedźwiecki *et al.*, "J-PET: A new technology for the whole-body PET imaging," *Acta Phys. Polon. B*, vol. 48, pp. 1567–1576, 2017.

[13] B. Hiesmayr and P. Moskal, "Genuine multipartite entanglement in the 3-photon decay of positronium," *Scientific Reports*, vol. 7, p. 15349, 2017.

[14] ——, "Witnessing entanglement in compton scattering processes via mutually unbiased bases," *Submitted*, 2018. [Online]. Available: https://arxiv.org/abs/1807.04934

[15] D. Kamińska *et al.*, "A feasibility study of ortho-positronium decays measurement with the J-PET scanner based on plastic scintillators," *Eur. Phys. J. C*, vol. 76, p. 445, 2016.

[16] P. Moskal, N. Krawczyk, B. Hiesmayr *et al.*, "Feasibility studies of the polarization of photons beyond the optical wavelength regime with the J-PET detector," *Eur. Phys. J. C*, vol. 78, p. 970, 2018.

[17] P. Moskal *et al.*, "Potential of the J-PET detector for studies of discrete symmetries in decays of positronium atom - a purely leptonic system," *Acta Phys. Polon. B*, vol. 47, pp. 509–535, 2016.

[18] M. Pawlik-Niedzwiecka *et al.*, "Preliminary studies of j-pet detector spatial resolution," *Acta Phys. Polon. A*, vol. 132, no. 5, 2017.

[19] L. Raczyński *et al.*, "Calculation of the time resolution of the j-pet tomograph using kernel density estimation," *Phys. Med. Biol.*, vol. 62, no. 12, pp. 5076–5097, 2017.

[20] G. Korcyl *et al.*, "Evaluation of single-chip, real-time tomographic data processing on fpga - soc devices," *IEEE Trans. Med. Im.*, vol. 31, no. 11, pp. 2526–2535, 2018.

[21] M. Palka *et al.*, "Multichannel fpga based mvt system for high precision time (20 ps rms) and charge measurement," *JINST*, vol. 12, p. P08001, 2017.

[22] P. Moskal, O. Rundel *et al.*, "Time resolution of the plastic scintillator strips with matrix photomultiplier readout for J-PET tomograph," *Phys. Med. Biol.*, vol. 61, pp. 2025–2047, 2016.

[23] P. Kowalski, W. Wiślicki, R. Shopa, L. Raczyński, K. Klimaszewski *et al.*, "Estimating the nema characteristics of the j-pet tomograph using the gate package," *Phys. Med. Biol.*, vol. 63, p. 165008, 2018.

[24] S. Jan *et al.*, "Gate v6: a major enhancement of the gate simulation platform enabling modelling of ct and radiotherapy," *Physics in Medicine & Biology*, vol. 56, no. 4, p. 881, 2011.

[25] Gate collaboration. [Online]. Available: http://www.opengatecollaboration.org/

[26] J. Allison *et al.*, "Geant4 developments and applications," *IEEE TNS*, vol. 53, no. 1, pp. 270–278, 2006.

[27] C. Robert *et al.*, "Distributions of secondary particles in proton and carbon-ion therapy: a comparison between gate/geant4 and fluka monte carlo codes," *Physics in Medicine & Biology*, vol. 58, no. 9, p. 2879, 2013.

[28] A. Rucinski *et al.*, "Commissioning and clinical validation of GPU-accelerated Monte Carlo code for proton beam therapy," *Submitted to Medical Physics*, 2018.

[29] E. Almhagen, D. J. Boersma, H. Nyström, and A. Ahnesjö, "A beam model for focused proton pencil beams," *Physica Medica*, vol. 52, pp. 27–32, 2018.